Journal of Manufacturing Processes 32 (2018) 93–99

Contents lists available at ScienceDirect

Journal of Manufacturing Processes

journal homepage: www.elsevier.com/locate/manpro

Microstructure and crystallization mechanism of Ti-based bulk metallic glass by electron beam welding

Gang Wang[a,b,*], Yongjiang Huang[c], Wei Cao[b], Zhongjia Huang[a], Marko Huttula[b], Yongsheng Su[a], Caiwang Tan[c]

[a] School of Mechanical and Automotive Engineering, Anhui Polytechnic University, Wuhu 241000, PR China
[b] Nano and Molecular Systems Research Unit, University of Oulu, P.O. Box 3000, FIN-90014, Oulu, Finland
[c] State Key Laboratory of Advanced Welding and Joining, Harbin Institute of Technology, Harbin 150001, PR China

ARTICLE INFO

Article history:
Received 7 November 2017
Received in revised form
11 December 2017
Accepted 28 January 2018

Keywords:
Bulk metallic glass
Electron beam welding
Weld zone
Heat affected zone

ABSTRACT

In this work, we report on the successful welding of the Ti-based bulk metallic glass (BMG) plates via electron beam welding route. Microstructure determination shows that crystalline phases exist both in weld zone (WZ) and heat affected zone (HAZ). The critical cooling rate for glass formation in WZ is depended on the solidification condition. The continuous heating transformation curve (CHT) of glass transition temperature (T_g) and crystallization temperature (T_x) during heating process, time-temperature-transformation diagram (C-curve) during cooling process, and the thermal cycle curves are obtained by Kissinger equation, nucleation theory, and temperature field simulation, respectively. The crystallization mechanism in HAZ was discussed in details during the heating and cooling processes. The intersection between cooling curve and C-curve denotes the crystallization of HAZ during the cooling process.

Introduction

Due to the disordered atomic structures inherited from molten melts, bulk metallic glasses (BMGs) are normally endowed with unusual physical, mechanical, and chemical properties superior to those of their crystalline counterparts. With high hardness, excellent corrosion resistance, superior strength, and high elastic limit, the BMGs are promising for multifunctional applications in different industries [1]. However, their three-dimensional (3D) size is limited within only tens of millimeters, yet, severely hindering the industrial applications of BMGs [2]. Thus, it is crucial to find a route to form bigger BMGs in order to enable them as structural materials.

To date, numerous efforts have been devoted to increase the 3D size of BMGs, including optimization of chemical composition and preparation technology, welding and 3D print process [3–9]. High energy beam welding, as a modern welding process, has been widely used because of its advantages such as deep welding penetration, high welding energy density, and little deformation and so on [10]. Yokoyama et al. connected the Zr-based metallic glass using a conventional electron-beam welding process [11]. Similarly, the Zr-based metallic glasses were tightly wielded by using a focused fiber laser beam [12]. Shen et al. successfully welded $Ti_{40}Zr_{25}Ni_3Cu_{12}Be_{20}$ BMG together by laser welding process, and found that the tensile strength of the welded sample can reach up to 93% of the base material [13]. Tsumaura et al. investigated dissimilar joining of Ni-based metallic glass to stainless steel by fiber laser beam [14]. Despite of these experimental studies, mechanisms towards crystallization kinetics and thermal stability have been scarcely reported. Chen et al. researched the crystallization behaviors of Zr-based BMG by Kissinger analysis and temperature field simulation [15]. Sun et al. demonstrated the spherulitic crystallization mechanism of BMG by activation energy and nucleation theory [16]. Lu et al. studied the crystallization of a Zr-based BMG during laser 3D printing process based on the thermal cycle curves obtained from finite element method (FEM) analysis [17]. It should be noticed that the crystallization mechanism in the aforementioned works has been only interpreted during either heating or cooling process. Therefore, it is necessary to propose an integral and effective method for crystallization analysis in both the heating and cooling processes.

In the present work, we used electron beam to weld the $Ti_{40}Zr_{25}Ni_3Cu_{12}Be_{20}$ BMG. The microstructure in the weld zone (WZ) and heat affected zone (HAZ) was studied in details. The continuous transformation heating curve (CHT) during heating process

* Corresponding author at: School of Mechanical and Automotive Engineering, Anhui Polytechnic University, Wuhu 241000, PR China.
E-mail addresses: gangwang@ahpu.edu.cn, wg10310918@163.com (G. Wang).

https://doi.org/10.1016/j.jmapro.2018.01.027
1526-6125/

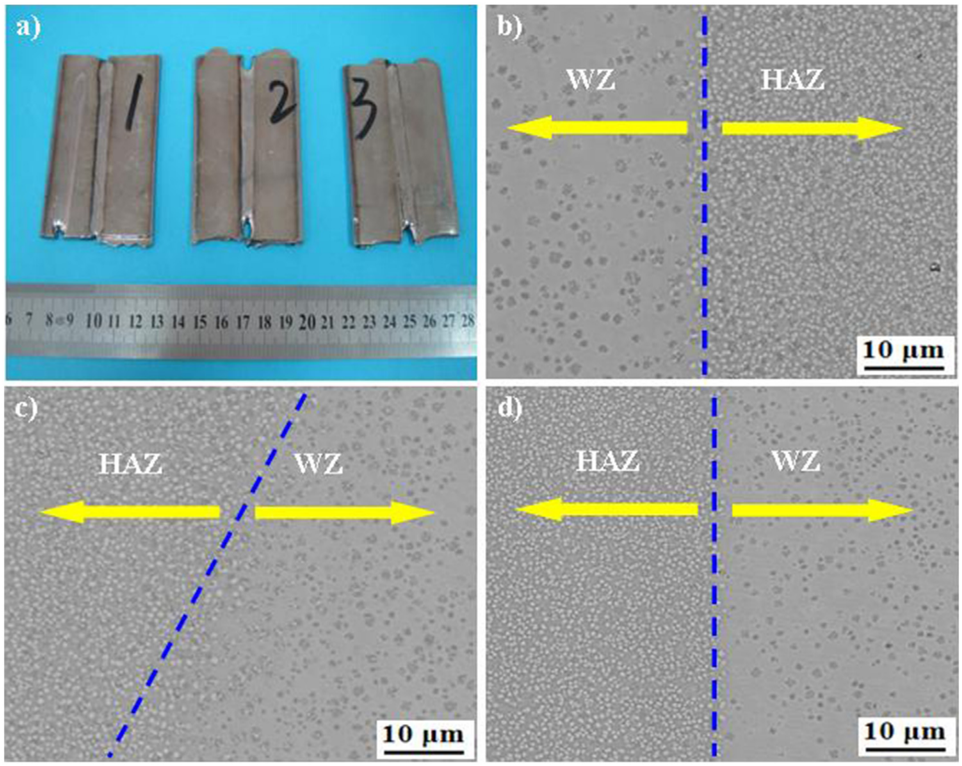

Fig. 1. a) Outer appearance of welded samples and SEM images of fusion zone in welded Ti-based BMG joint with different welding speeds: (b) 28 mm/min, (c) 32 mm/min, and (d) 34 mm/min.

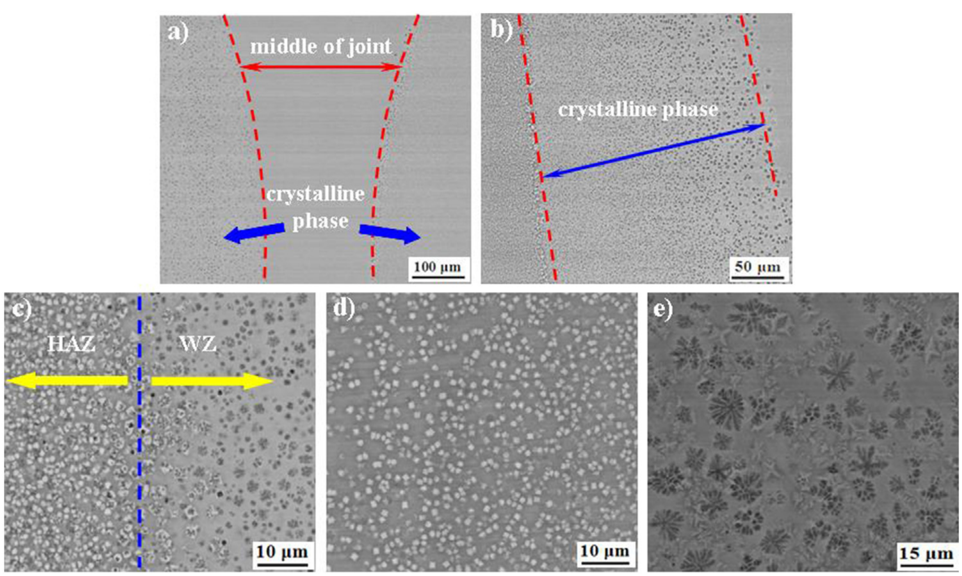

Fig. 2. SEM images of welded Ti-based joint with a welding speed of 34 mm/s: a) middle of the weld, b) WZ, c) fusion zone, d) HAZ, and e) magnification of WZ.

and time-temperature-transformation diagram (C-curve) during cooling process were obtained by Kissinger equation and nucleation theory. Also, the thermal cycle curves with different welding parameters were obtained by temperature field simulation. By combining these curves, the crystallization mechanisms in HAZ were proposed for both heating and cooling process.

Experimental

The quinary $Ti_{40}Zr_{25}Ni_3Cu_{12}Be_{20}$ alloy ingots were prepared by arc melting Ti, Zr, Ni, Cu, and Be metals with purities above 99.9% and drop casting into a copper mould in a Ti-gettered argon atmosphere. The obtained plate-shaped samples had a dimension of 3 mm × 30 mm × 50 mm. The glassy nature of the as-cast samples was confirmed by X-ray diffraction analysis. The electron-beam welding was carried out in a vacuum of 5×10^{-3} Pa. The accelerate voltage was 150 kV and the focus current was 2057 mA. The welding beam current was 16 mA. The welding speeds ranged from 28 mm/s to 34 mm/s, respectively. The ratio of the focal length and distance from specimen surface to electron lens, a_b value, was selected to be 1. After welding, microstructure observations were conducted by scanning electron microscopy (SEM, Quanta